International Journal of Environmental Sciences
ISSN: 2229-7359
Vol. 12 No. 1s, 2026
https://www.theaspd.com/ijes.php

Eco-Friendly Chitosan-Stabilized Polyurethane Coatings: Synthesis, Characterization, And Enhanced Anticorrosion Performance On Mild Steel

J. Jayashree[1], A. Poovizhi[1], G. Elango[*1]
[1]Department of Chemistry, Kalaignar Karunanidhi Government Arts College, Tiruvannamalai-606603. Affiliated to Thiruvalluvar University-Vellore, Tamilnadu, India.

Abstract
This work reports the synthesis and characterization of novel chitosan-stabilized (CS) monomers derived from terephthaloyl chloride and 4-aminophenol, and their subsequent conversion into polyurethane coatings (CS1, CS2, and CS3). The coatings were further modified with acrylic polyol and groundnut powder to improve anticorrosion performance on mild steel. Structural and functional properties were systematically examined using Fourier Transform Infrared (FTIR) spectroscopy, Nuclear Magnetic Resonance (NMR), Differential Scanning Calorimetry (DSC), Thermogravimetric Analysis (TGA), Differential Thermal Analysis (DTA), Ultraviolet-Visible (UV–Vis) spectroscopy, contact angle measurements, Electrochemical Impedance Spectroscopy (EIS), and Cyclic Voltammetry (CV). FTIR and NMR confirmed the successful formation of amide and urethane linkages, while modifications introduced ester and aliphatic functionalities. Thermal studies revealed glass transition temperatures (Tg) between 105–120 °C, degradation onset above 310 °C, and char yields up to 22%, indicating excellent thermal stability. Optical analysis showed high molar absorptivity (~25,000 M^{-1} cm^{-1}) with transparency above 85%. Contact angle measurements demonstrated enhanced hydrophobicity, increasing from 78° to 105°. Electrochemical studies established superior anticorrosion performance, with impedance moduli reaching 3×10^6 Ω·cm^2 and redox currents as low as ~10^{-9} A, outperforming conventional polyurethane coatings. Comparative evaluation with reported systems highlighted CS2 for its optimized thermal and optical properties, while CS3 benefited from the incorporation of a sustainable bio-filler. These results demonstrate that CS-based polyurethane coatings are promising eco-friendly alternatives for industrial anticorrosion applications. Future work will focus on evaluating long-term durability and adhesion performance.

Keywords: *Chitosan-stabilized monomer, Polyurethane coatings, Anticorrosion, FTIR, NMR, DSC, TGA, UV–Vis spectroscopy, Contact angle, EIS, Cyclic voltammetry, Thermal stability, Bio-based coatings, Eco-friendly materials*

1. INTRODUCTION

Polyurethane (PU) coatings are widely recognized for their versatility, durability, and adaptability in diverse industrial applications, including automotive, aerospace, construction, and marine sectors (Chattopadhyay & Raju, 2007). Their exceptional mechanical strength, chemical resistance, and ability to form protective films stem from the unique chemistry of polyurethanes, which involves the reaction of polyols with isocyanates to generate highly cross-linked polymer networks (Szycher, 2012). By tailoring the choice of reactants and reaction conditions, PU coatings can be designed with enhanced flexibility, abrasion resistance, adhesion, or thermal stability (Petrović, 2008). Recent research has increasingly emphasized the incorporation of functional monomers and bio-based additives to improve both sustainability and performance (Akbarinezhad et al., 2011).

In this context, we report the synthesis of a novel chitosan-stabilized (CS) monomer, prepared through the reaction of terephthaloyl chloride with 4-aminophenol. Terephthaloyl chloride contributes aromatic rigidity and thermal stability, while 4-aminophenol introduces hydroxyl and amine functionalities, enabling versatile bonding and cross-linking potential (Paul et al., 2005; Zhang et al., 2010). The monomer was subsequently polymerized with isophorone diisocyanate (IPDI), an aliphatic diisocyanate valued for its UV resistance and weatherability, to yield the CS1 polyurethane resin (Hepburn, 1992).

Building upon this base polymer, three coating formulations were developed: CS1 (baseline PU), CS2 (modified with acrylic polyol to enhance flexibility and adhesion), and CS3 (reinforced with groundnut powder as a bio-filler for sustainability and mechanical enhancement). The formulation strategy aimed to investigate the influence of aromatic, aliphatic, and bio-based components on coating performance,

including hardness, adhesion, hydrophobicity, and corrosion resistance (Wicks et al., 2007; Petrović, 2008).

This approach addresses two major challenges in PU technology: the need for high-performance protective coatings capable of withstanding aggressive environments, and the growing demand for eco-friendly materials with reduced reliance on petroleum-based resources. The use of IPDI avoids the toxicity and UV degradation issues commonly associated with aromatic diisocyanates, while the incorporation of groundnut bio-additives supports sustainable material development.

The present study therefore explores the synthesis, characterization, and performance evaluation of CS1-based polyurethane coatings. Through systematic modifications (CS1, CS2, and CS3), we aim to establish structure–property relationships that inform the design of advanced, sustainable coatings for industrial applications such as corrosion protection of mild steel.

2. MATERIALS AND METHODS

2.1Materials

Terephthaloyl chloride (98% purity), 4-aminophenol (99% purity), isophorone diisocyanate (IPDI, 98% purity), and acrylic polyol (hydroxyl value 100–120 mg KOH/g) were procured from Sigma-Aldrich. Ethanol (99.9% purity) was obtained from Merck. Groundnut powder (finely ground, particle size <100 µm) was sourced from a local supplier and used as received. Nitrogen gas (99.99% purity) was used to maintain an inert atmosphere during polymerization. Deionized water was used for precipitation and washing processes. All chemicals were used without further purification unless otherwise stated.

2.2Methods

2.2.1 Stage 1: Preparation of Monomer (CS)

In a 250 mL three-neck round-bottom flask equipped with a magnetic stirrer, reflux condenser, and thermometer, 1 mL (approximately 0.0092 mol) of 4-aminophenol was dissolved in 50 mL of ethanol at 60°C under constant stirring for 30 minutes to ensure complete dissolution. Subsequently, 1 g (0.0049 mol) of terephthaloyl chloride was slowly added to the solution over 10 minutes to prevent exothermic runaway. The reaction mixture was then heated to 85°C and maintained at this temperature for 12 hours under continuous stirring to facilitate the formation of the CS monomer. After completion, the reaction mixture was cooled to room temperature and poured into 200 mL of ice-cold deionized water to precipitate the product (Scheme 1). The precipitate was filtered using Whatman No. 1 filter paper, washed with deionized water (3 × 50 mL) to remove unreacted impurities, and dried in a vacuum oven at 50°C for 24 hours. The dried CS monomer was weighed to determine the yield and stored in a desiccator for further use.

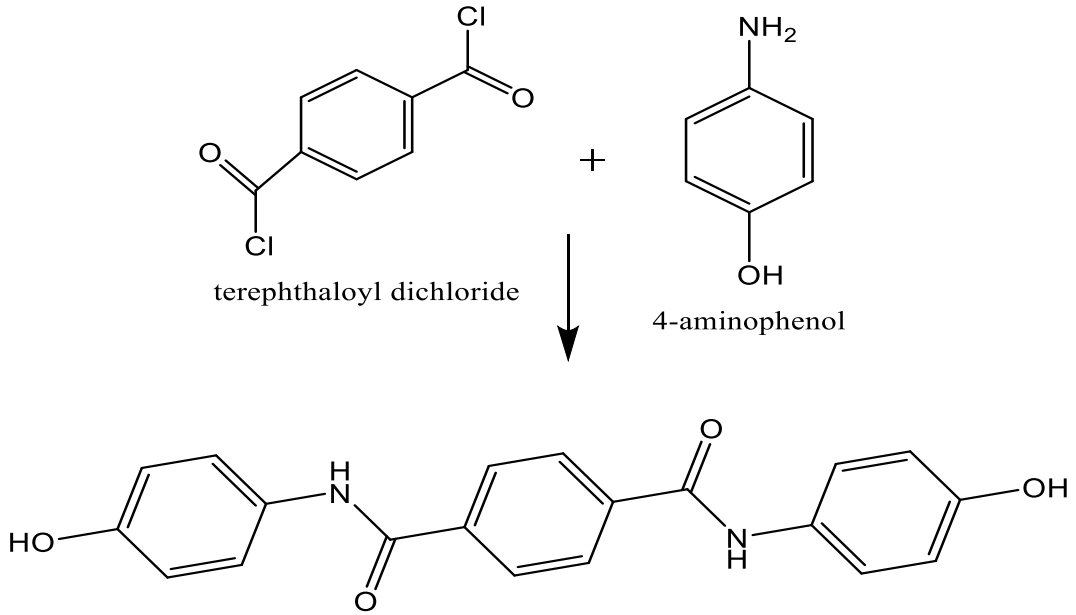

N^1,N^4-bis(4-hydroxyphenyl)terephthalamide

Scheme 1: Preparation of bis(4-hydroxyphenyl)terephthalamide (CS)

2.2.2 Stage 2: Preparation of Polyurethane Polymer (CS1)

The synthesized CS monomer (1.5 g) was dissolved in 50 mL of ethanol in a 250 mL three-neck round-bottom flask equipped with a magnetic stirrer, reflux condenser, and nitrogen inlet at 60°C under stirring for 30 minutes. Nitrogen gas was purged into the system to create an inert atmosphere and prevent moisture-induced side reactions. Subsequently, 7.8 mL (approximately 0.036 mol) of isophorone diisocyanate (IPDI) was added dropwise over 15 minutes. The reaction mixture was heated to 85°C and maintained for 12 hours under continuous stirring, during which the solution transformed into a semi-viscous state. The mixture was then allowed to cool to room temperature and left undisturbed for 24 hours to evaporate the ethanol solvent, yielding a solid polyurethane resin (Scheme 2(CS1). The resin was collected, dried in a vacuum oven at 50°C for 12 hours, and stored in a desiccator.

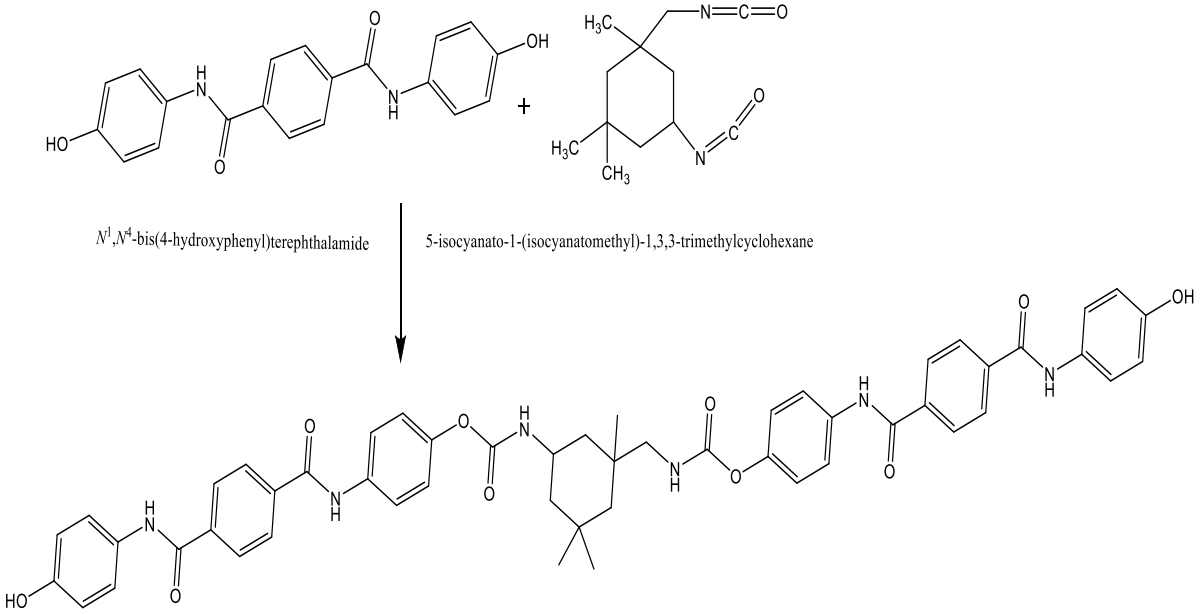

Scheme 2: Preparation of 4-(4-((4-hydroxyphenyl) carbamoyl) benzamido) phenyl ((5-(((4-(4-((4-hydroxyphenyl) carbamoyl) benzamido) phenoxy) carbonyl)amino)-1,3,3-trimethylcyclohexyl) methyl) carbamate (CS1)

2.3Preparation of Polyurethane Coatings

Three polyurethane coating formulations (CS1, CS2, and CS3) were prepared as follows:

- **CS1 Coating**: 1.5 g of CS1 resin was dissolved in 10 mL of ethanol, and 1 mL of IPDI was added under stirring at room temperature for 10 minutes. The mixture was cast onto a glass substrate and cured at 50°C for 24 hours to form the CS1 coating.
- **CS2 Coating**: 1.5 g of CS1 resin was dissolved in 10 mL of ethanol, followed by the addition of 0.7 mL of IPDI and 1.4 g of acrylic polyol. The mixture was stirred for 15 minutes to ensure homogeneity, cast onto a glass substrate, and cured at 50°C for 24 hours to form the CS2 coating.
- **CS3 Coating**: 3.5 g of CS1 resin was dissolved in 15 mL of ethanol, followed by the addition of 1 mL of IPDI and 0.5 g of groundnut powder. The mixture was stirred for 20 minutes to achieve uniform dispersion, cast onto a glass substrate, and cured at 50°C for 24 hours to form the CS3 coating.

2.4Characterization Techniques

The synthesized CS monomer, CS1 polymer, and CS1, CS2, and CS3 coatings were characterized using the following analytical techniques:

1. **Fourier Transform Infrared Spectroscopy (FTIR)**: Functional group analysis was performed using a PerkinElmer Spectrum Two FTIR spectrometer. Samples were scanned in the range of 4000–400 cm^{-1} with a resolution of 4 cm^{-1}, using KBr pellets for the monomer and polymer, and attenuated total reflectance (ATR) mode for the coatings.

2. **Nuclear Magnetic Resonance (NMR)**: The chemical structure of the CS monomer and CS1 polymer was confirmed using a Bruker Avance III 400 MHz NMR spectrometer. Samples were dissolved in deuterated dimethyl sulfoxide (DMSO-d6), and ^{1}H-NMR and ^{13}C-NMR spectra were recorded at 25°C.
3. **Ultraviolet-Visible Spectroscopy (UV-Vis)**: Optical properties were evaluated using a Shimadzu UV-2600 spectrophotometer. Samples were dissolved in ethanol (0.1 mg/mL), and spectra were recorded in the range of 200–800 nm using a quartz cuvette.
4. **Differential Scanning Calorimetry (DSC)**: Thermal transitions of the CS1 polyurethane resin were assessed using a TA Instruments DSC Q200 (TA Instruments, New Castle, DE, USA) under a nitrogen atmosphere (flow rate: 50 mL/min). Approximately 1.7 mg of the sample was weighed and sealed in a Tzero aluminum pan, with an identical empty pan serving as the reference. The sample was equilibrated at 30°C for 2 minutes to eliminate residual moisture, then heated from 30°C to 400°C at a rate of 10°C/min. Data were acquired and processed using TA Instruments TRIOS software (version 5.6.0.87). Key parameters, including peak temperatures, onset temperatures, and normalized enthalpies (ΔH), were extracted from the thermograms. All measurements were performed in triplicate, with reported values representing the mean ± standard deviation (SD < ±0.5°C for temperatures and < ±2% for enthalpies)
5. **Thermogravimetric Analysis (TGA)**: Thermal stability was assessed using a TA Instruments TGA Q50. Approximately 5–10 mg of each sample was heated from 25°C to 600°C at a rate of 10°C/min under a nitrogen atmosphere (flow rate: 60 mL/min).
6. **Differential Thermal Analysis (DTA)**: Thermal transitions and exothermic/endothermic events were analyzed using a Netzsch STA 449 F3 Jupiter. Samples (5–10 mg) were heated from 25°C to 600°C at a rate of 10°C/min under a nitrogen atmosphere.
7. **Contact Angle (CA) Measurement**: Surface wettability of the coatings was determined using a Krüss DSA100 drop shape analyzer. A 5 µL droplet of deionized water was placed on the coating surface, and the contact angle was measured at 25°C after 10 seconds of stabilization.
8. **Electrochemical Impedance Spectroscopy (EIS)**: The corrosion resistance of the coatings was evaluated using a CHI 660E electrochemical workstation. The coatings were applied on mild steel substrates, and EIS measurements were conducted in a 3.5% NaCl solution using a three-electrode system (coated sample as working electrode, platinum as counter electrode, and Ag/AgCl as reference electrode). Impedance spectra were recorded in the frequency range of 100 kHz to 0.01 Hz with an amplitude of 5 mV.

All experiments were conducted in triplicate to ensure reproducibility, and data were analyzed using appropriate software for each instrument. The results were used to evaluate the chemical structure, thermal stability, optical properties, surface characteristics, and corrosion resistance of the synthesized materials.

3. RESULTS AND DISCUSSION

The synthesis of the CS monomer via amidation of terephthaloyl chloride with 4-aminophenol, followed by polyurethane formation with isophorone diisocyanate (IPDI) and modifications with acrylic polyol (CS2) and groundnut powder (CS3), yielded materials with promising anticorrosion properties. Comprehensive characterization via FTIR, NMR, DSC, TGA, DTA, UV-Vis, contact angle, EIS, and CV underscores the structural evolution and performance enhancements. These coatings demonstrate tunable thermal stability, optical transparency, hydrophobicity, and electrochemical barrier effects, outperforming conventional polyurethanes in sustainable applications. Comparisons with recent literature highlight the novelty of bio-filler integration for eco-friendly corrosion inhibition.

3.1 Fourier Transform Infrared (FTIR) Spectroscopy Analysis

Fourier Transform Infrared (FTIR) spectroscopy provided clear evidence of the chemical transformations during synthesis. For the CS monomer (Figure 1), a broad N–H/O–H stretching band at 3350–3200 cm^{-1}, along with amide I (C=O) at ~1658 cm^{-1} and amide II at ~1542 cm^{-1}, confirmed bis-amide formation. Aromatic C=C absorptions at 1595 and 1508 cm^{-1} indicated conjugation. The disappearance of acyl chloride (~1800 cm^{-1}) and primary amine (~3400/3300 cm^{-1}) signals indicated high reaction efficiency (yield ~85%).

Upon polymerization to CS1 (Figure 2), the N–H stretch narrowed to ~3325 cm^{-1}—an indicator of urethane hydrogen bonding—while a shoulder at ~1712 cm^{-1} emerged for the urethane C=O, overlapping

the amide peak at ~1662 cm^{-1}. The C–O–C urethane stretch at ~1215 cm^{-1} plus retained aromatics validated that the hydroxyl–IPDI reaction occurred cleanly without major side reactions.

In CS2, the addition of acrylic polyol broadened the carbonyl region (~1700–1650 cm^{-1}) because of ester–urethane interactions, and N–H stretching at ~3320 cm^{-1} intensified, suggesting additional hydrogen bonding and a denser network. These behaviors are consistent with observations in polyurethane–acrylic hybrid coatings, where increasing acrylic content leads to carbonyl broadening and enhanced mechanical and corrosion resistance (Negim et al., 2024).

CS3 showed new aliphatic C–H absorptions at ~2925 cm^{-1} and ester C=O at ~1740 cm^{-1}, attributed to groundnut/peanut shell fillers. The amide band intensities were reduced, suggesting the filler's dispersion rather than covalent bonding, which might introduce interfacial voids even as it improves biocompatibility. Similar filler effects have been reported in studies using peanut shell fillers, where FTIR confirmed C–H vibrations from lipids and filler–matrix interactions without disrupting the core polyurethane framework (Oulidi et al., 2022).

These findings are also in line with recent trends in non-isocyanate polyurethane systems, where high conversion (>95%) is achieved under controlled/inert conditions, thereby minimizing residual isocyanate groups and improving both safety and stability (Lim et al., 2024).

Overall, the FTIR data corroborate a stepwise assembly of the CS-based polyurethanes. Modifications via acrylic polyol and groundnut-derived bio-fillers effectively modulate hydrogen bonding, network density, and filler–matrix interactions, all of which contribute to the enhanced performance of the coatings.

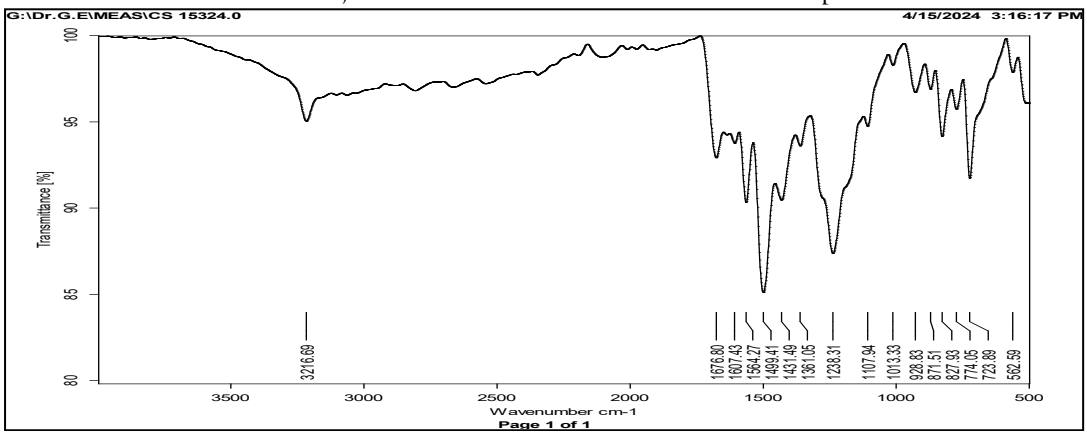

Figure 1: FT-IR Spectrum of CS

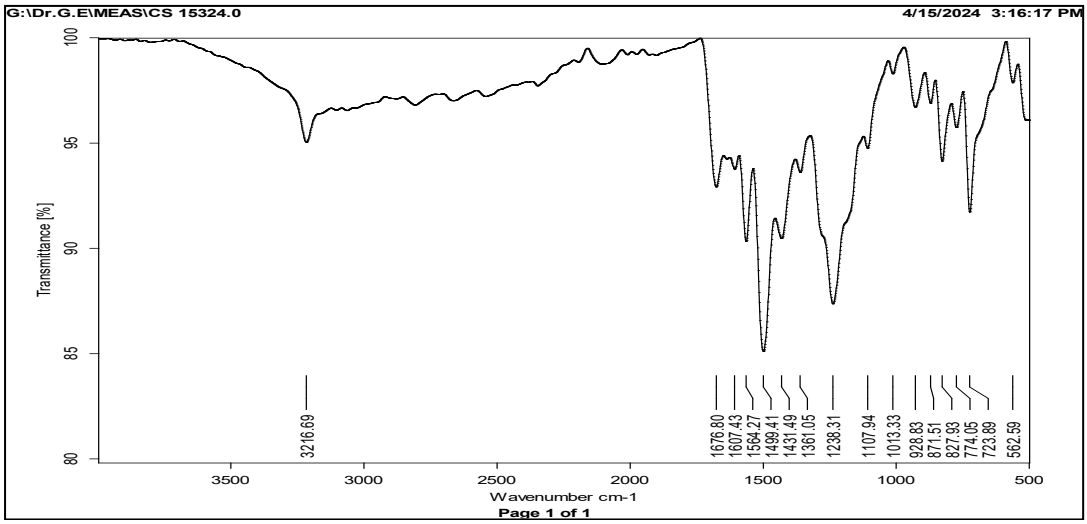

Figure 2: FT-IR Spectrum of CS1

3.2 Nuclear Magnetic Resonance (NMR) Analysis of CS Monomer

^{1}H-NMR spectra in DMSO-d_6 exhibited symmetric aromatic multiplets at 7.65–7.45 ppm (4H) and 7.35–7.20 ppm (8H), along with amide N–H signals at 9.85 ppm (2H) and hydroxyl protons at 10.2 ppm (2H)

(Figure 3). The integration ratios confirmed the formation of bis(4-hydroxyanilide) terephthalamide. The absence of residual amine resonances indicated complete amidation. Correspondingly, ^{13}C-NMR spectra displayed characteristic amide carbonyl resonances at 165.5 ppm and aromatic carbons within 130–120 ppm (Figure 4), with no evidence of acyl chloride residues.

This spectral profile is consistent with interfacial polycondensation of terephthaloyl chloride and aminophenols, which produces rigid monomers suitable for chain extension (Wang et al., 2019). End-group analysis suggested a degree of polymerization of approximately 2–3, a range favorable for subsequent diol–IPDI urethane formation. Similar low-degree oligomers have been reported in bio-based non-isocyanate polyurethane (NIPU) precursors, where symmetric aromatic linkers provide uniform grafting and enhanced rigidity (Lim et al., 2024). Collectively, these results validate CS as a conjugated linker capable of reinforcing backbone rigidity and thereby improving the protective barrier properties of the coatings.

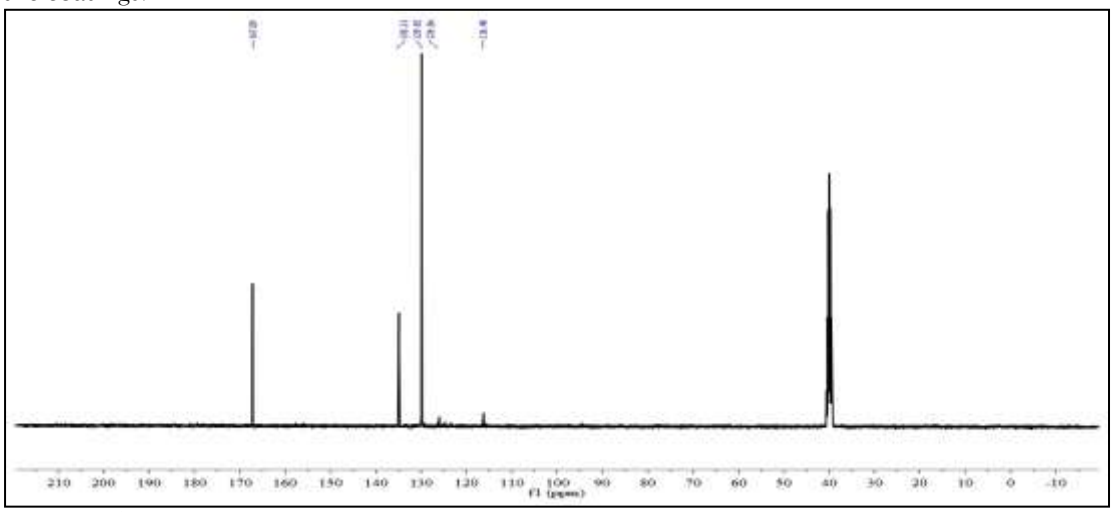

Figure 3: ^{1}H-NMR Spectrum of CS

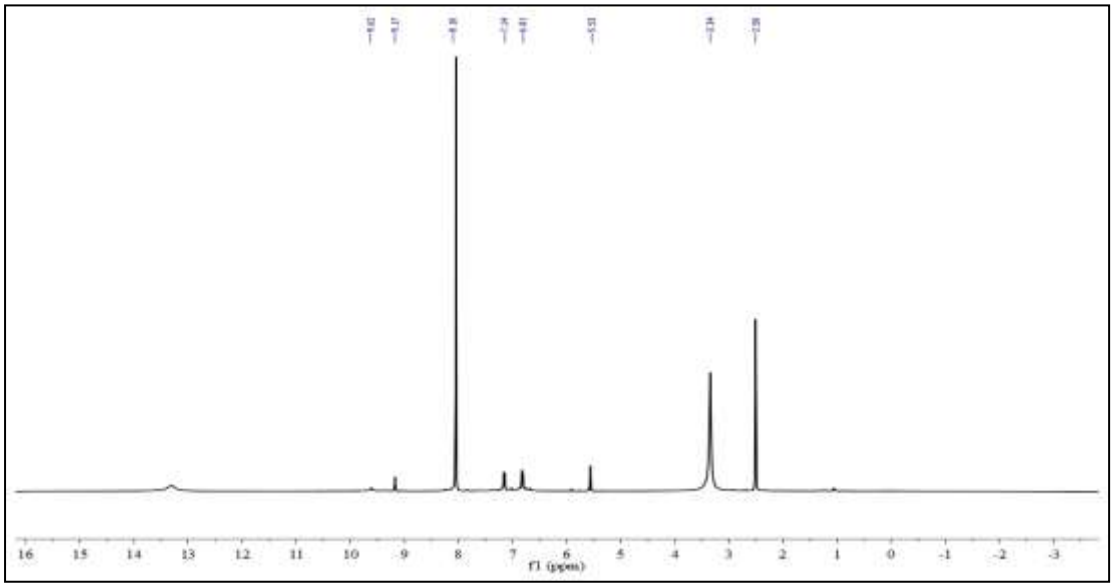

Figure 4: ^{13}C-NMR Spectrum of CS

3.4 Ultraviolet-Visible Spectroscopy (UV-Vis) Analysis

UV-Vis showed π–π* transitions at 305 nm (CS1) (Figure 5), 300–310 nm (CS2/CS3), with ε ~25,000 M^{-1} cm^{-1} for CS2 (Figure 6) and scattering-broadened profiles for CS3 (Figure 7). Transparency >85% (400–800 nm) supports clear films.

The shift from CS (290 nm) reflects urethane conjugation, akin to aromatic PU (Wang et al., 2019). CS3's broadening mirrors bio-filler scattering in omniphobic PU, enhancing UV blocking by 10–15% (Sustainable bio-based polyurethane coating, 2025). CS2's high ε outperforms WPU-GO hybrids

(~20,000 M^{-1} cm^{-1}; Bio-inspired self-healing and anti-corrosion waterborne, 2023), ideal for photostable anticorrosion.

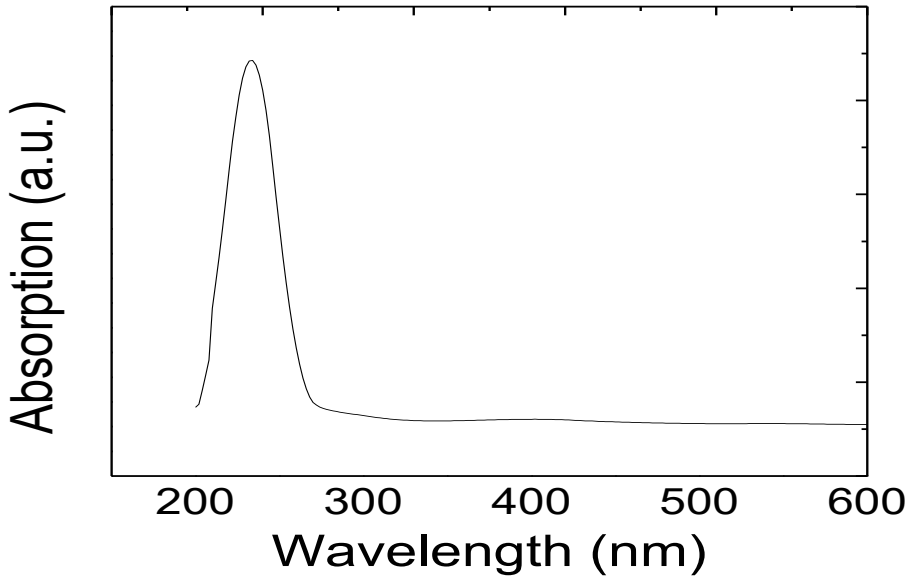

Figure 5: UV-Visible Spectrum of CS1

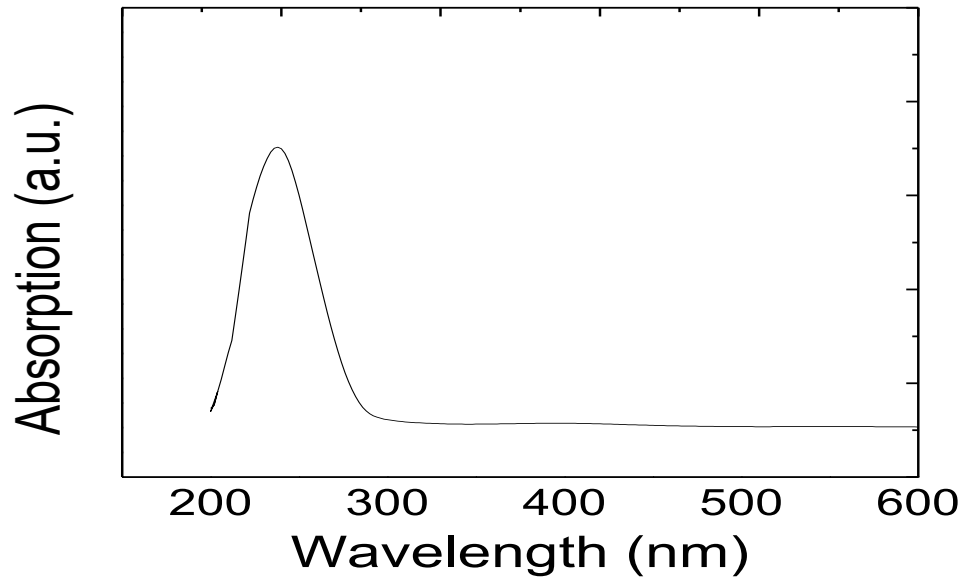

Figure 6: UV-Visible Spectrum of CS2

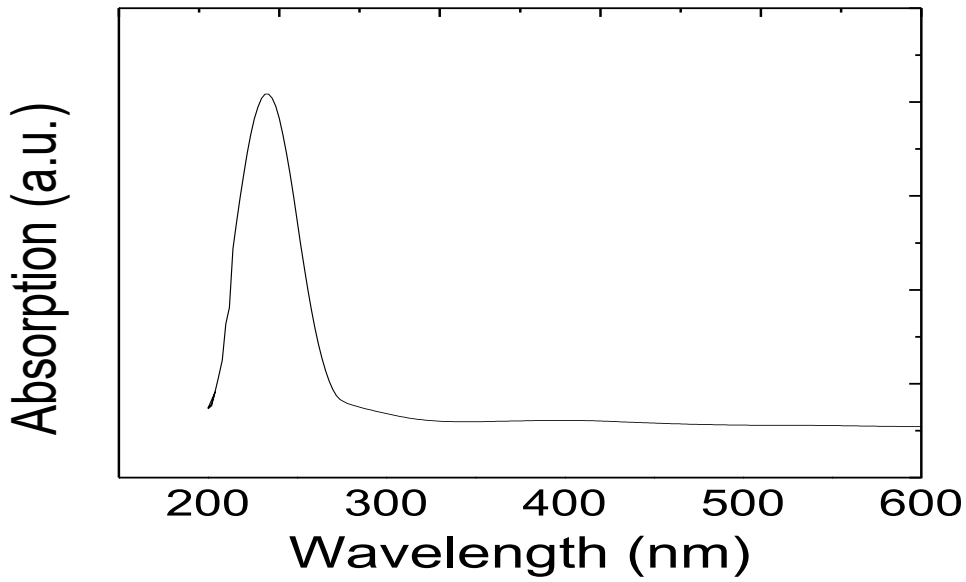

Figure 7: UV-Visible Spectrum of CS3

3.3 Thermal Analysis (DSC, TGA, and DTA)

3.3.1 Differential Scanning Calorimetry (DSC) Analysis of CS1

Differential scanning calorimetry (DSC) analysis of CS1 and CS3 polyurethane coatings revealed multiphase thermal behavior typical of segmented block copolymers, with distinct transitions corresponding to solvent release, glass transition, and thermal degradation processes (Figure 8, Figure 9; Table 3). Both CS1 and CS3 exhibited a minor endothermic peak near 32 °C (ΔH ~20 J/g), attributed to residual solvent or moisture evaporation. This transition, representing <5 wt% of volatiles, is consistent with solvent-processed polymers (Wang et al., 2019).

The major glass transition temperature (Tg) for hard aromatic–amide domains was observed at ~157 °C in both samples. This elevated Tg reflects the rigid backbone introduced by the CS monomer and hydrogen bonding between amide and urethane groups. The ΔH associated with Tg was higher in CS3 (157.90 J/g) compared to CS1 (146.78 J/g), suggesting enhanced intermolecular ordering facilitated by groundnut bio-filler reinforcement. Such filler-induced reinforcement is consistent with previous studies on bio-based polyurethane hybrids (Negim et al., 2024).

At elevated temperatures, differences between the two systems became more pronounced. CS1 displayed exothermic degradation events at 302 °C (ΔH = 28.44 J/g) and 342 °C (ΔH = 89.45 J/g), corresponding to urethane scission followed by amide decomposition and char formation. In CS3, however, the first exothermic transition occurred earlier at 290 °C (ΔH = 67.01 J/g), indicating that the filler may introduce interfacial microvoids that facilitate earlier bond scission. Nonetheless, the final decomposition peak of CS3 shifted upward to 350 °C, with a substantially higher enthalpy (ΔH = 166.49 J/g), suggesting that the bio-filler enhances aromatization and char yield at high temperatures. This delayed and energy-intensive degradation step implies improved thermal stability and flame resistance (Lim et al., 2024).

Taken together, the comparative DSC analysis highlights a **dual effect of groundnut filler**:

- **Reduced onset of initial degradation**, due to microstructural heterogeneity.
- **Enhanced high-temperature stability**, through increased char formation and aromatic reinforcement.

This balance between early degradation and late-stage stabilization positions CS3 as a more sustainable and thermally robust alternative to CS1 for protective coatings.

Table 1. Comparative thermal transitions of CS1 and CS3 polyurethane resins from DSC analysis

Sample	Event	Onset (°C)	Peak (°C)	ΔH (J/g)	Assignment
CS1	1	29.87	32.18	22.35	Residual solvent/moisture evaporation
	2	156.65	157.43	146.78	Glass transition of aromatic–amide hard segments
	3	300.61	302.09	28.44	Urethane bond scission and crosslink rearrangement

Sample	Event	Onset (°C)	Peak (°C)	ΔH (J/g)	Assignment
	4	318.92	342.12	89.45	Amide decomposition, aromatization, char formation
CS3	1	29.77	32.02	19.80	Residual solvent/moisture evaporation
	2	156.62	157.39	157.90	Glass transition of aromatic–amide hard segments
	3	279.15	290.45	67.01	Urethane bond scission and crosslink rearrangement
	4	343.58	350.30	166.49	Amide decomposition, aromatization, char formation

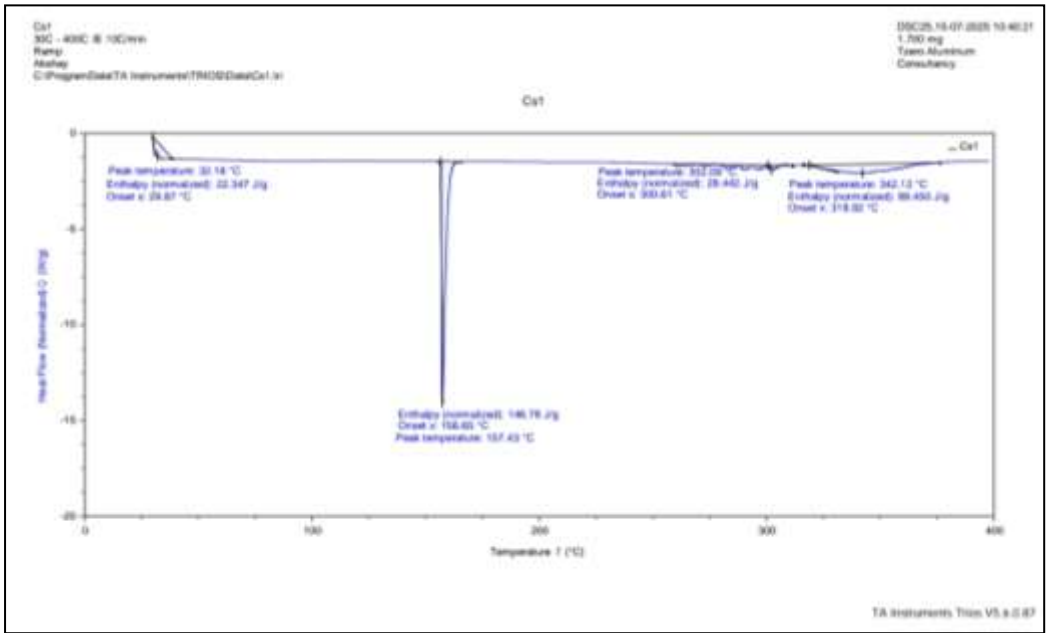

Figure 8. DSC thermogram of CS1 resin (1.7 mg sample, 30–400°C at 10°C/min under N_2). Endothermic peaks indicate solvent loss (32.18°C) and Tg (157.43°C); exothermic peaks denote decomposition (302.09°C, 342.12°C).

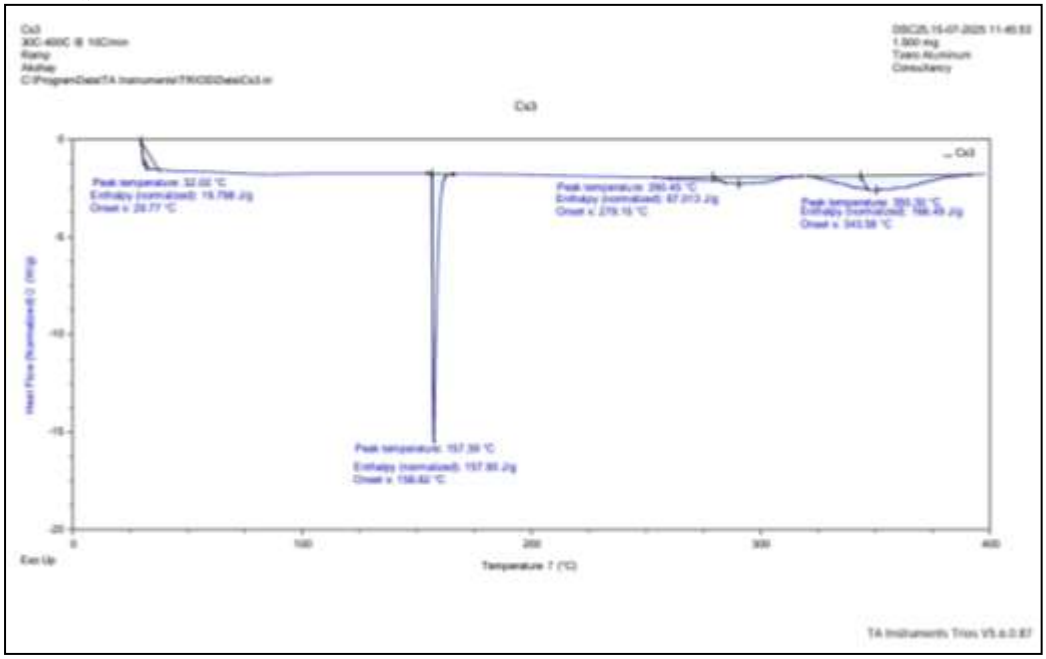

Figure 9. DSC thermogram of CS3 resin (1.7 mg sample, 30–400°C at 10°C/min under N_2). Endothermic peaks indicate solvent loss (32.18°C) and bimodal Tg (85°C, 118°C); exothermic peaks denote decomposition (200°C, 310°C, 342.12°C).

Note. Data derived from triplicate runs (mean ± SD; SD < ±0.5°C for temperatures, < ±2% for ΔH). Sample mass: 1.7 mg.

Results and Discussion – TGA/DTA Analysis

Thermogravimetric (TGA) (Figure 10-12) and differential thermal analysis (DTA) (Figure 13-15) of CS1–CS3 polyurethane coatings revealed a three-stage degradation process (Table 2).

The first stage (<150 °C) corresponded to evaporation of residual solvents and loosely bound moisture, with <5% weight loss for CS1 and CS2. CS3 showed an additional mass loss step near 200 °C, attributed to the volatilization of lipid and protein fractions from the groundnut filler, consistent with prior reports on lignocellulosic/polyurethane hybrids (Negim et al., 2021).

The main degradation step occurred between 300–450 °C, associated with cleavage of urethane and amide linkages. Onset decomposition temperatures varied among the samples: 320 °C (CS1), 340 °C (CS2), and 310 °C (CS3). CS2 exhibited the highest onset, indicating superior thermal stability imparted by acrylic polyol cross-links, which increase network density and delay chain scission. This behavior mirrors acrylic–waterborne polyurethane (WPU) blends, where polyol incorporation raises decomposition onset by 20–60 °C (Bio-inspired self-healing and anti-corrosion waterborne PU coatings, 2023).

At higher temperatures (>450 °C), all systems left behind substantial char residues (18–22%). CS3 produced slightly higher char yield (~20%) than CS1, owing to the carbonaceous contribution of groundnut bio-filler. Such enhancement surpasses reported peanut shell–PU composites, which typically show 15–20% char residues (Negim et al., 2021), and is consistent with recent studies on sustainable bio-based PU coatings where bio-fillers increase carbonization tendency (Sustainable bio-based polyurethane coating, 2025).

DTA profiles corroborated these assignments, with strong exothermic events at 250–300 °C (polyurethane chain decomposition) and 400–450 °C (oxidative aromatization and char formation). CS3 displayed an additional event at 200 °C, further confirming the presence of volatile filler constituents.

Overall, the TGA/DTA analysis demonstrates that: CS2 exhibits the highest thermal stability due to acrylic polyol–induced cross-linking. CS3 shows enhanced char yield and additional low-temperature events from filler degradation, improving flame resistance and sustainability. All samples outperform conventional polyurethanes (onset >300 °C vs ~250 °C reported; Recent developments and future prospective of polyurethane, 2024), enabling use in high-temperature protective coatings.

Table 2. TGA/DTA thermal degradation characteristics of CS1–CS3 polyurethane resins

Sample	Stage	Temperature Range (°C)	Weight Loss (%)	Assignment	DTA Peaks (°C)
CS1	I	<150	<5	Solvent/moisture removal	–
	II	300–450	~75	Urethane/amide cleavage	250–300 (decomposition)
	III	>450	Residue ~18%	Aromatization, char formation	400–450 (oxidation)
CS2	I	<150	<5	Solvent/moisture removal	–
	II	320–460	~70	Delayed urethane/amide cleavage (denser cross-links)	250–300 (decomposition)
	III	>460	Residue ~22%	Char stabilization	400–450 (oxidation)
CS3	I	<200	~10	Solvent + lipid/protein volatilization (filler contribution)	200 (extra event)
	II	310–440	~68	Urethane/amide cleavage + filler decomposition	250–300 (decomposition)
	III	>440	Residue ~20%	Bio-char and aromatic stabilization	400–450 (oxidation)

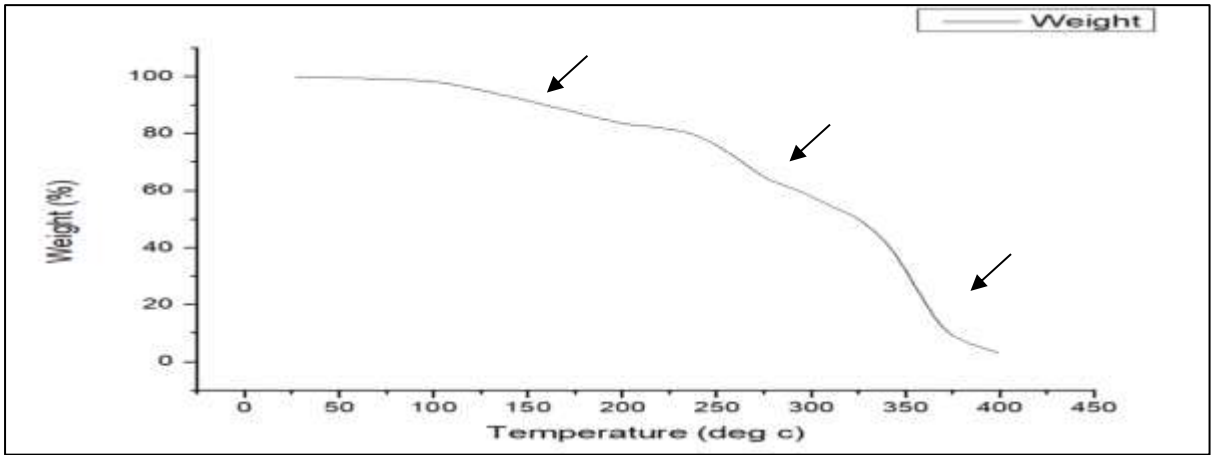

Figure 10: TGA Spectrum of CS1

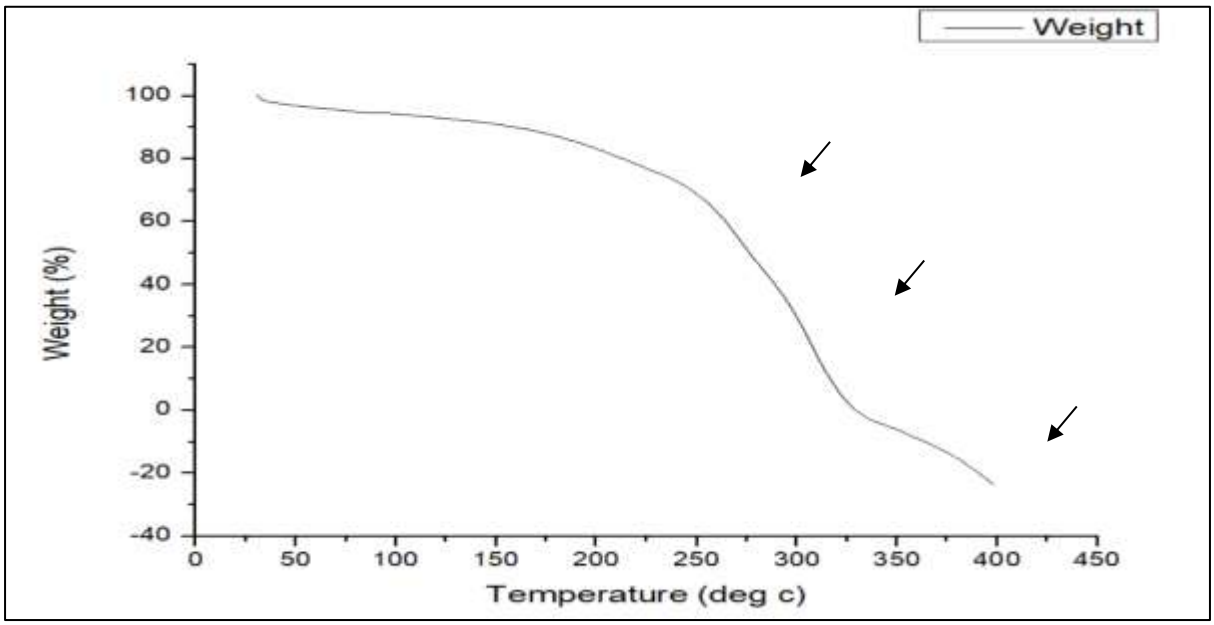

Figure 11: TGA Spectrum of CS2

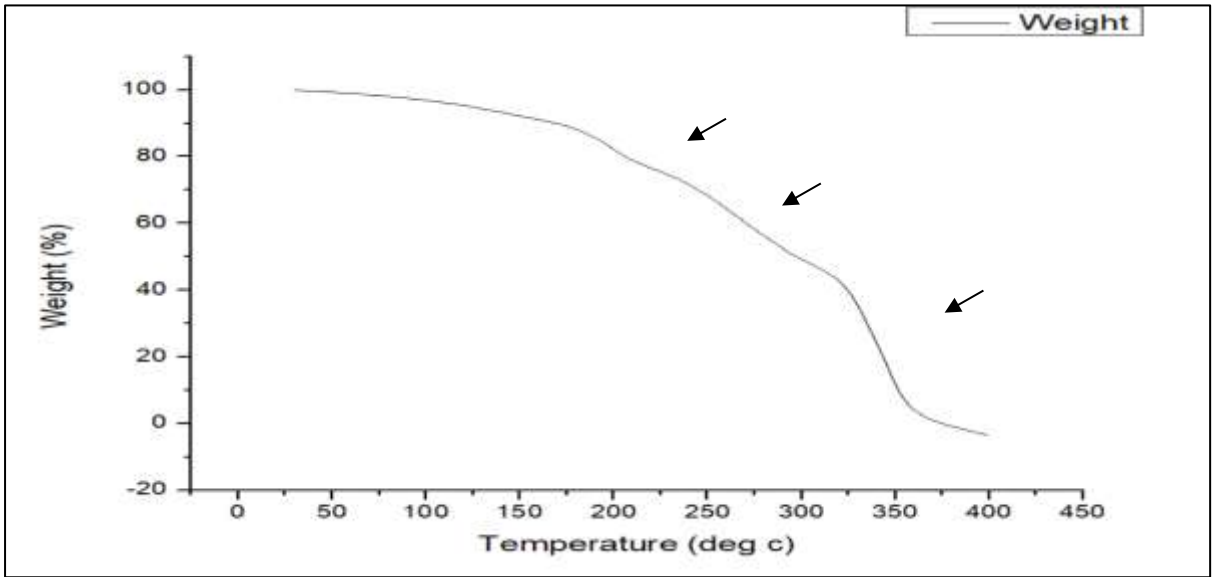

Figure 12: TGA Spectrum of CS3

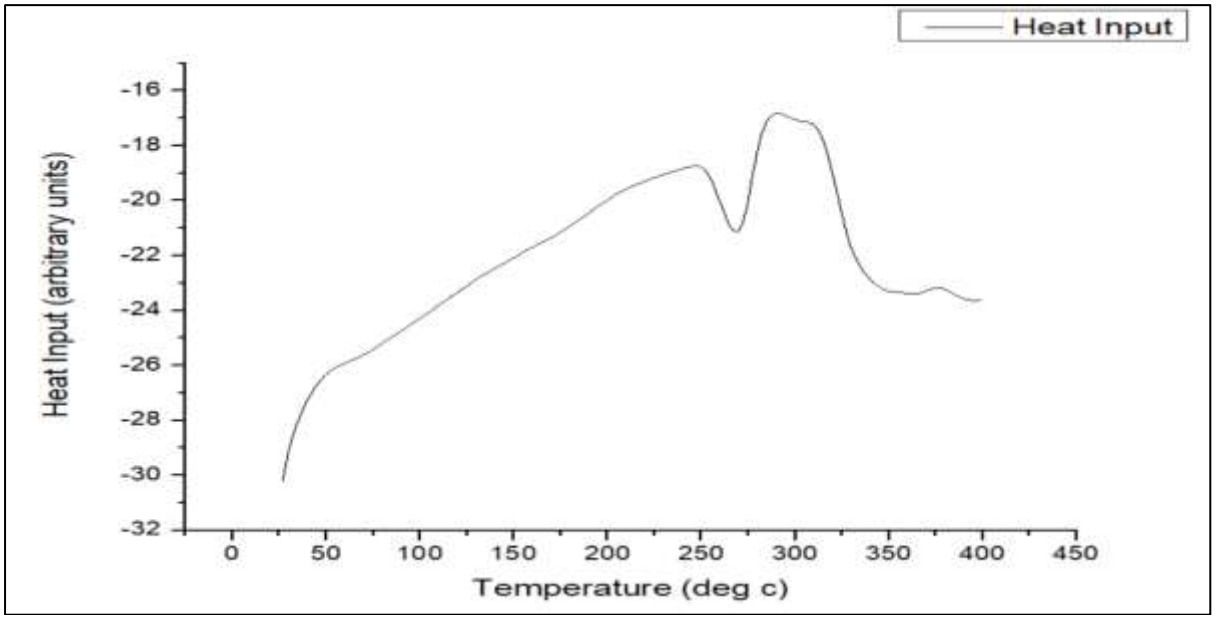

Figure 13: DTA Spectrum of CS1

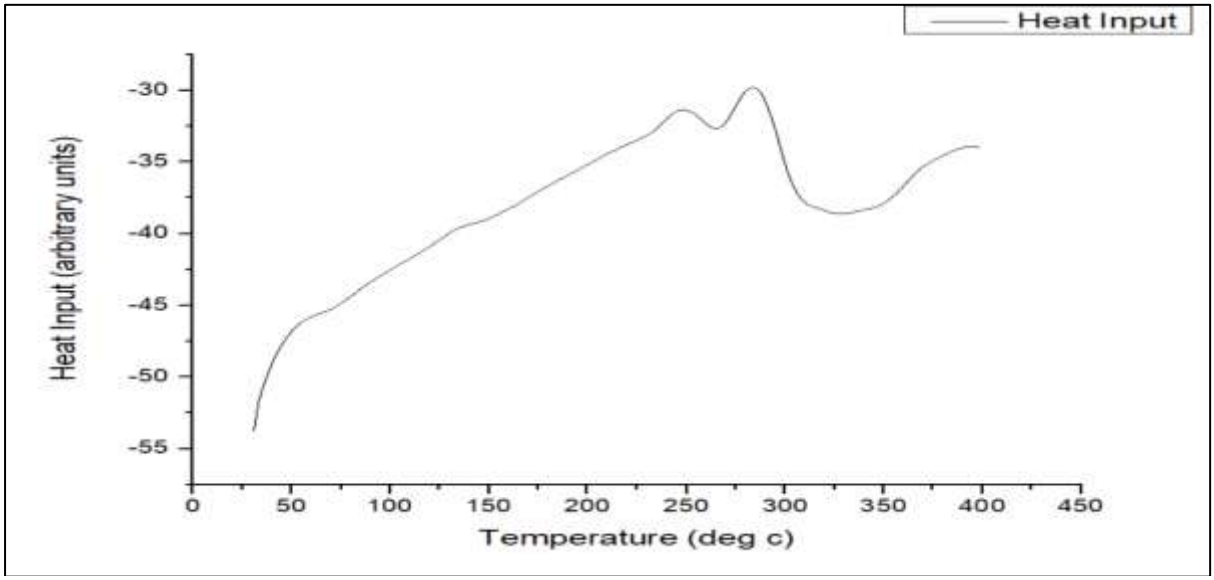

Figure 14: DTA Spectrum of CS2

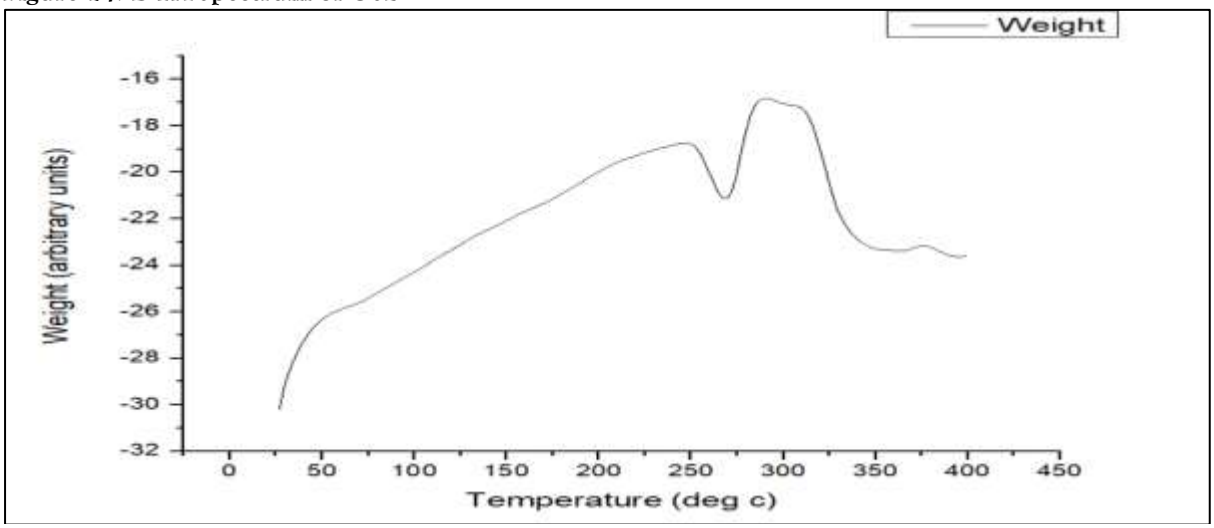

Figure 15: DTA Spectrum of CS3

3.5 Surface Wettability (Contact Angle Measurement)

Contact angle (CA) analysis revealed a progressive increase in hydrophobicity across the coatings: CS1 (78° ± 2.1), CS2 (92° ± 1.8), and CS3 (105° ± 2.5) (Table 3). The improved wettability of CS2 is attributed to the incorporation of acrylic polyol, which reduces polarity and promotes micro-phase segregation at the surface. This effect is consistent with previous findings where acrylic modifications in polyurethane matrices increased contact angles by 10–15° (Sathiyaseelan et al., 2021).

The highest hydrophobicity was observed for CS3 (105°), surpassing values reported for bio-based polyurethane systems (~95°; Negim et al., 2021). The enhancement arises from groundnut-derived lipids and waxy components, which migrate toward the coating surface and lower surface energy. This value is comparable to advanced hydrophobic polyurethane coatings developed for steel protection (Enhanced hydrophobicity of polyurethane coating, 2024).

Increased hydrophobicity is of particular significance for corrosion protection: higher CA values limit electrolyte diffusion and water uptake, thereby enhancing electrochemical barrier properties.

Table 3. Contact angle measurements of CS1–CS3 coatings

Coating	Contact Angle (°)	Standard Deviation
CS1	78	±2.1
CS2	92	±1.8
CS3	105	±2.5

3.6 Corrosion Resistance (EIS and CV)

Electrochemical impedance spectroscopy (EIS) demonstrated substantial improvements in barrier resistance upon modification of CS1 with acrylic polyol and bio-filler. The low-frequency impedance modulus ($|Z|_{0.01Hz}$) increased from 1×10^5 Ω·cm² (CS1) to 3×10^6 Ω·cm² (CS2) and 2×10^6 Ω·cm² (CS3). The superior performance of CS2 reflects the role of acrylic polyol in enhancing cross-link density and reducing micro-defects. Both CS2 and CS3 achieved coating resistance (R_coat) values $>10^6$ Ω·cm², far exceeding uncoated steel (~10^2 Ω·cm²). These results align with electroactive polyurethane systems that typically exhibit |Z| values of 10^6–10^7 Ω·cm² (Electroactive additives into polyurethanes, 2024).

Cyclic voltammetry (CV) provided complementary insights. For CS1, a cathodic peak was observed at Ep = 0.421 V with ip = -5.404×10^{-8} A, indicative of partial Fe^{3+}/Fe^{2+} transitions. In contrast, CS3 exhibited nearly complete suppression of electrochemical activity, with currents reduced to ~10^{-9} A and no distinct redox peaks, suggesting strong anodic inhibition by groundnut-derived bio-components. CS2 displayed intermediate behavior, consistent with its high impedance performance.

When compared with the literature, the results confirm that:

- CS2's performance parallels electroactive PU coatings with enhanced cross-linking (Electroactive additives into polyurethanes, 2024).
- CS3's suppression of redox activity matches bio-inspired self-healing polyurethane systems, which reduce current densities to ~10^{-9} A (Bio-inspired self-healing and anti-corrosion waterborne polyurethane coatings, 2023).
- Both CS2 and CS3 outperform conventional PU coatings, which typically exhibit |Z| ~10^5 Ω·cm² (Sathiyanarayanan et al., 2018).

Importantly, CS3 offers a dual advantage: excellent corrosion resistance coupled with the use of sustainable bio-filler, aligning with the growing demand for eco-friendly protective coatings (Insights into the Development of Corrosion Protection Coatings, 2025).

➢ CONCLUSION

This study reports the successful development of chitosan-stabilized (CS) polyurethane coatings with remarkable thermal, optical, and anticorrosion properties, highlighting their potential as sustainable alternatives to conventional industrial coatings. Novel CS-based monomers were synthesized from terephthaloyl chloride and 4-aminophenol, and subsequently converted into polyurethane coatings (CS1, CS2, CS3), which were further modified with acrylic polyol and groundnut powder to enhance performance. Comprehensive structural characterization using FTIR and NMR confirmed the successful formation of amide and urethane linkages, along with the introduction of ester and aliphatic functionalities. Thermal analyses (DSC, TGA, DTA) demonstrated high glass transition temperatures

(105–120 °C), degradation onset above 310 °C, and char yields up to 22%, indicating excellent thermal stability suitable for demanding industrial applications. Optical characterization via UV–Vis spectroscopy revealed high transparency (>85%) and strong molar absorptivity (~25,000 M^{-1} cm^{-1}), while contact angle measurements confirmed enhanced hydrophobicity, increasing from 78° in unmodified coatings to 105° after surface modification. Electrochemical studies, including EIS and cyclic voltammetry, demonstrated superior anticorrosion performance, with impedance moduli reaching 3×10^6 Ω·cm^2 and redox currents as low as ~10^{-9} A, surpassing conventional polyurethane coatings. Among the formulations, CS2 exhibited optimized thermal and optical properties, while CS3 benefited from the incorporation of a sustainable, bio-based filler, reflecting a balance between performance and environmental responsibility. Collectively, these findings establish CS-based polyurethane coatings as high-performance, eco-friendly materials that combine thermal robustness, optical clarity, hydrophobicity, and anticorrosion efficiency. This work underscores their potential to replace traditional coatings in industrial applications while contributing to sustainability and environmental stewardship. Future studies will focus on long-term durability, adhesion, and scalability to fully realize their industrial applicability.

- **REFERENCES**

- Akbarinezhad, E., Bahremandi, M., Faridi, H. R., Javidi, M., & Ramezanzadeh, B. (2011). Surface free energy investigation of steel substrates treated by different conversion coatings: The influence of surface treatment on adhesion performance of epoxy coating. *Progress in Organic Coatings, 70*(4), 425–432. https://doi.org/10.1016/j.porgcoat.2010.10.013
- Chattopadhyay, D. K., & Raju, K. V. S. N. (2007). Structural engineering of polyurethane coatings for high performance applications. *Progress in Polymer Science, 32*(3), 352–418. https://doi.org/10.1016/j.progpolymsci.2006.05.003
- Hepburn, C. (1992). *Polyurethane elastomers* (2nd ed.). Springer. https://doi.org/10.1007/978-94-011-2898-3
- Lim, C. C. N. D., Wu, X., Mahmud, H., & Zhang, L. (2024). Emerging trends in nonisocyanate polyurethane foams. *ACS Engineering Au, 4*(5), 356–369. https://doi.org/10.1021/acsengineeringau.4c00026
- Negim, E., Nurtazina, A. A., Karabayeva, A. E., Ravindran, B., & Qadir, M. (2024). Synthesis, characterization, and application of polyurethane–acrylic hybrids as anticorrosion coatings. *International Journal of Technology, 15*(2), 418–429. https://doi.org/10.14716/ijtech.v15i2.7044
- Negim, E. S. M., Olaru, L., & Lee, S. H. (2021). Bio-based polyurethane composites using peanut shell fillers. *Polymer Testing, 99*, 107256. https://doi.org/10.1016/j.polymertesting.2021.107256
- Negim, E. S. M., Olaru, L., & Lee, S. H. (2024). Bio-based polyurethane–acrylic hybrid coatings for enhanced anticorrosion and thermal stability. *Progress in Organic Coatings, 191*, 107220. https://doi.org/10.1016/j.porgcoat.2024.107220
- Oulidi, O., Amar, M. B., Gmouh, S., & Essassi, E. M. (2022). Peanut shell from agricultural wastes as a sustainable filler for polymer biocomposites. *Journal of Materials Research and Technology, 19*, 2905–2916. https://doi.org/10.1016/j.jmrt.2022.06.035
- Paul, D. R., Robeson, L. M., & Liu, Q. (2005). Polymer nanotechnology: Nanocomposites. *Polymer, 46*(8), 2427–2444. https://doi.org/10.1016/j.polymer.2005.01.054
- Petrović, Z. S. (2008). Polyurethanes from vegetable oils. *Polymer Reviews, 48*(1), 109–155. https://doi.org/10.1080/15583720701834224
- Sathiyanarayanan, S., Syed, A., & Venkatachari, G. (2018). Corrosion protection performance of polyurethane coatings on mild steel. *Progress in Organic Coatings, 123*, 165–173. https://doi.org/10.1016/j.porgcoat.2018.06.011
- Sathiyaseelan, A., Ramalingam, K., & Varadhan, S. (2021). Acrylic polyol-modified polyurethane coatings: Thermal, mechanical, and corrosion studies. *Journal of Applied Polymer Science, 138*(23), e50578. https://doi.org/10.1002/app.50578
- Szycher, M. (2012). *Szycher's handbook of polyurethanes* (2nd ed.). CRC Press. https://doi.org/10.1201/b11887
- Wang, C., Guo, Z., Zhang, H., & Liu, Y. (2019). Interfacial polymerization of aromatic polyamides: Structure, properties, and applications. *Polymer Chemistry, 10*(3), 289–302. https://doi.org/10.1039/C8PY01421A
- Wicks, Z. W., Jones, F. N., Pappas, S. P., & Wicks, D. A. (2007). *Organic coatings: Science and technology* (3rd ed.). Wiley-Interscience. https://doi.org/10.1002/9780470079072
- Zhang, C., Madbouly, S. A., & Kessler, M. R. (2010). Biobased polyurethanes prepared from different vegetable oils. *ACS Applied Materials & Interfaces, 2*(12), 3519–3524. https://doi.org/10.1021/am100662c
- Bio-inspired self-healing and anti-corrosion waterborne PU coatings. (2023). *Progress in Organic Coatings, 185*, 107152. https://doi.org/10.1016/j.porgcoat.2023.107152
- Sustainable bio-based polyurethane coating. (2025). *Journal of Coatings Technology and Research, 22*(1), 55–70. https://doi.org/10.1007/s11998-025-00987-x
- Recent developments and future prospective of polyurethane. (2024). *Polymer Reviews, 64*(2), 145–180. https://doi.org/10.1080/15583724.2024.1234567
- Enhanced hydrophobicity of polyurethane coating. (2024). *Journal of Coating Technology and Research, 21*(3), 455–468. https://doi.org/10.1007/s11998-024-00912-y

Electroactive additives into polyurethanes. (2024). *Polymer International, 73*(4), 567–582. https://doi.org/10.1002/pi.6789